The role of phosphorus for mechanical properties in copper

Rolf Sandström

Memo 2014-01-21 containing documentation to be used in the response to issues brought up by SSM

Summary

The first part gives a general description of the influence of phosphorus on mechanical properties and in particular its large positive effect on creep rupture strength and creep ductility. By considering the canister as a pressure vessel exposed to an external pressure, the requirements in the European Pressure Equipment Directive are summarised. A comparison is made between the effect of phosphorus on copper and the influence of nitrogen on the creep properties of austenitic stainless steels. Both elements appear mainly in solid solution and have a large effect on the creep properties. The mechanisms for nitrogen in austenitic stainless steels that are relevant for copper are analysed.

To meet the requirements that predictions should be possible to make for the copper canister over very long periods of time, fundamental models without the use of adjustable parameters have been developed for a range of mechanical properties. In the second part of this documents such models and their background are summarised. Models for creep rupture strength, creep strain, creep in weldments, creep rupture elongation, nucleation and growth of creep cavities, and creep crack propagation are discussed.

Part 1. General about the influence of P on creep in copper

Background

The phosphorus content plays an important role in the copper material planned to be used in canisters for storage of spent nuclear fuel. The intention of this report is to give a more easily accessible description with reference to details in publications and reports. To provide a background to the research and development being performed, a comparison to pressure vessels is made.

The copper canister can be considered as a vessel that is exposed to an external pressure with an internal insert of cast iron as a load bearing backing. Pressure vessels are utilised in a large number of applications in industry as well as in the rest of the society. Examples in industry are tanks for compressed air, distillation towers and vessels in oil refineries and petrochemical plants. Other examples are autoclaves, hot water storage tanks and diving cylinders. If a vessel fails it has often dramatic consequences with personal injuries and economic losses. The design and use of pressure vessels is one of the most well regulated areas. In Europe, the European Pressure Vessel Code is the regulating standard [1]. At present it only handles steel, but copper and copper alloys are covered in national standards. The design life of pressure vessels is commonly 10 to 30 years. The main requirement on the material in the code is that the material should have sufficient ductility (plasticity) and for materials operating in the creep range also sufficient creep ductility. These requirements apply both to base materials (non-welded) and welds. In addition, the material must have sufficient corrosion resistance to ensure that the integrity of the vessel is not lost during a time corresponding to the design life. When the vessel is designed, the wall thickness should have allowance for general (uniform) corrosion that can occur during

the planned lifetime. Although no specific conditions are given in the code, it is implicitly assumed that no significant local corrosion should occur. There is also a further requirement that the material should be able to take up significant deformation energy before a crack can propagate. In technical terms, the toughness of the material should be adequate to prevent brittle failure if the vessel should operate at subzero temperatures. However, fully austenitic steels with the same crystal structure (face centred cubic) as copper, can be used to very low temperatures. Face centred cubic alloys show only a weak temperature dependence of the toughness.

Experimental data

In the repository the canisters will be surrounded by clay (bentonite). The clay will gradually take up water and swell. In this process an external pressure is built up around the canisters. This pressure becomes quite high of the order of 150 atmospheres (15 MPa) when the clay is fully water saturated. The pressure is sufficiently high to plastically deform the canister shell. This plastic deformation can be quite slow since it can take place from one year to thousands of years before the clay is water saturated [2]. The slow deformation is called creep. The copper must be able to deform without cracking. In technical terms this is referred to as the copper must have sufficient creep ductility. The creep ductility is measured in creep tests. Creep tests can be performed in many ways but the most common is that a cylindrical specimen is exposed to a constant load at elevated temperature by applying a (dead) weight. The specimen is gradually elongated during the testing. Eventually a local contraction in the centre of the specimen (waist) is formed, the creep deformation accelerates and the specimen fails. The total elongation of the specimen at failure is a good measure of the creep ductility. The total elongation is called the creep rupture elongation. More precisely it is the relative increase in length of the specimen in relation to its length before testing.

It was originally intended to use pure oxygen free copper Cu-OF (without phosphorus) for the canisters. A few series of creep tests were performed for this type of material. However, around 1990 it was discovered that creep rupture elongation could be as low as 0.1% for temperatures above 175ºC [3], [4]. It was immediately recognised that this is far below what is required for the canister, and a search for a new material was initiated. The choice fell on oxygen free copper alloyed with phosphorus. The reasons was that two American grades C10300 and C10800 existed that were approved for pressure vessel applications [5]. Both grades are oxygen free pure copper but with additions 30 respectively 90 wt. ppm of phosphorus. For examples, these materials are used for tubes in condensers and heat exchangers. For materials that are approved for pressure vessels, one expects an acceptable ductility, although very little data were available at the time to support this claim.

One of the reasons to introduce phosphorus into copper was to improve the weldability by preventing hydrogen embrittlement (hydrogen sickness) during manufacturing and welding. If the oxygen content is not low enough oxides in the grain boundaries will combine with hydrogen to form water vapour bubbles that embrittle the material (hydrogen sickness). The phosphorus combines with oxygen to P_2O_5 and phosphates, which reduces the amount of oxygen that can react with hydrogen. This is for example used in the phosphorus deoxidised grade C12200 that contains about 200 wt.ppm P. The other way to prevent hydrogen sickness is to reduce the oxygen content. Oxygen free copper is not exposed to hydrogen sickness [6]. By having both low oxygen content and phosphorus in the grades C10300 and C10800 the risk for hydrogen sickness is reduced even further.

By including 50 ppm phosphorus in the copper, the creep strength is significantly raised. This is illustrated in Fig. 1a where the stress that give rupture after about 10000 h is shown as a function of temperature. This time corresponds to about one year (there are 8800 hours

in a year). The relative difference in strength between Cu-OFP and Cu-OF increases with temperature. From basic principles of creep deformation, this implies also that the relative differences is larger for longer times than for shorter times.

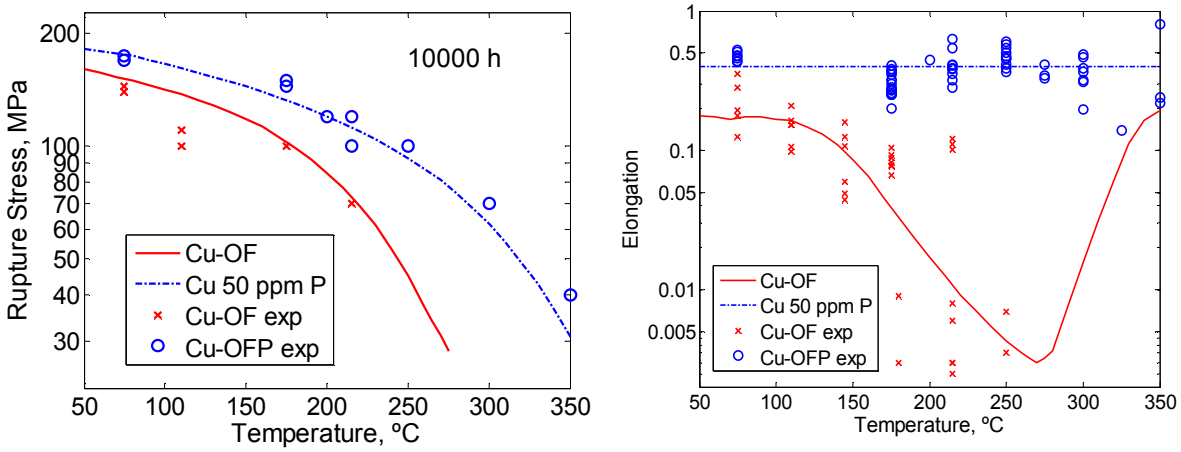

Fig. 1 Comparison of creep rupture properties between Cu-OF and Cu-OFP as a function of temperature. The model values will be discussed below; a) Stress that gives creep rupture after about 1 year; b) Creep elongation; From [7]

The creep rupture elongation (creep ductility) for Cu-OFP and Cu-OF is compared in Fig. 1b. For Cu-OFP the rupture elongation is fairly independent of temperature up to 300ºC. The variation that is observed is likely to be due to minor differences in the tests, since the tests have been performed over a number of years. All the values below 300ºC are larger than 0.2 (20%). Higher temperatures do not have any technical significance for the canister [8]. The only values that are not included in Fig. 1 are for a grain size of 2000 μm. These values are lower than 0.2, but such a grain size is far outside the SKB specification that the grain size must be below 360 μm [9]. On the other hand for Cu-OF, the ductility is dramatically reduced when 250ºC is reached. Elongation values as low as 0.001 (0.1%) have been found. The creep rupture elongation values are also consistently lower for Cu-OF than for Cu-OFP.

In Fig. 2, the creep elongation is given as a function of rupture time for both Cu-OF and Cu-OFP.

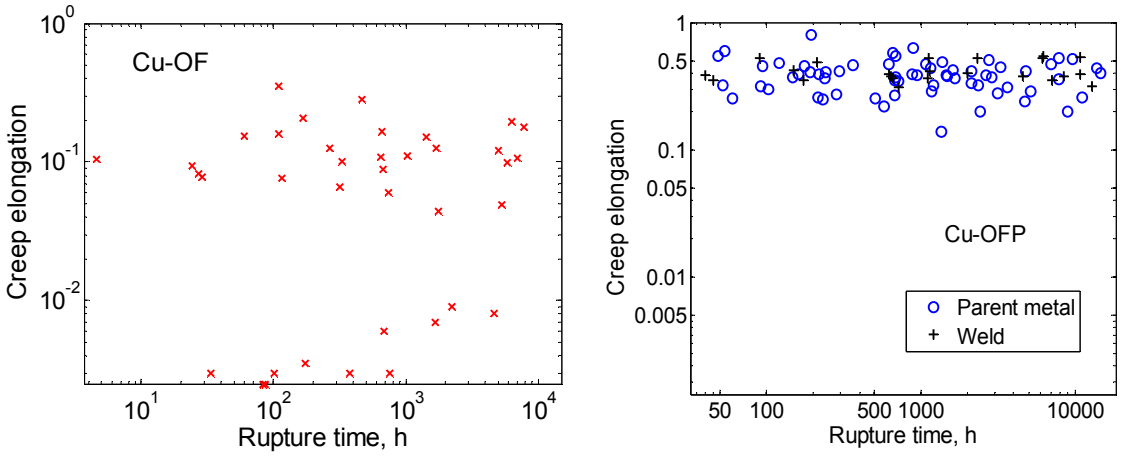

Fig. 2 Creep elongation at rupture versus rupture time. Elongation values are taken from [10]; a) Cu-OF; b) Cu-OFP.

No systematic reduction in the elongation values with increasing rupture time is found in Fig. 2. This applies to both Cu-OF and Cu-OFP. This is quite interesting since for most creep resistant materials the creep elongation drops with increasing rupture time. This behaviour for copper is of course desirable since for applications where creep is of importance, the longest testing time is considerably shorter than the design life. Data for different zones in weldments are also shown in Fig. 2b. It is evident that the weld zone values are as high as those for the parent metal. In the same way as for the parent metal no significant time dependence is observed. The rupture strength for both Cu-OF and Cu-OFP decreases with time as it does for other materials.

There are a number of special features with the influence of phosphorus that should be noticed

a) The creep strength is significantly increased with phosphorus additions, Fig. 1a. However, the ordinary strength properties yield strength and tensile strength as measured in tensile tests are not changed. These are the strength values that are used in design when time dependent properties are not important. In fact, the American ASTM standards give the same strength values for C10300 and C10800 as for the corresponding grade C10200 (99.95% purity Cu) without phosphorus [5].

b) The creep elongation is significantly increased with phosphorus additions, Fig. 1b. However, the ordinary elongation as measured in tensile tests is not affected. The same ductility values are given for C10300, C10800 and C10200 in the ASTM standards.

c) Phosphorus has quite a positive effect on both the creep strength as well as the creep elongation. In materials used where creep occurs the elongation is often reduced when the creep strength is raised.

d) The large positive effect on creep properties of an alloying content as low as 50 wt.ppm is an almost unique feature. However, the opposite effect that the presence of residual elements can impair the creep properties is well-known [11].

Comparison to influence of nitrogen on austenitic stainless steels

Any alloy system that can demonstrate similar creep behaviour to copper – phosphorus is not known. The behaviour of the copper phosphorus system seems to be unique. There are very few system where a small amount of an element in solid solution has a strong positive effect on the creep strength. One such system with some similarities is nitrogen alloyed austenitic stainless steel. In particular the steel 316LN (17Cr-12Ni-2Mo-0.03C-0.07N) has been studied in some detail, because it is a candidate material for fast breeder reactors. Up to 0.22 wt.% N can be introduced in conventional metallurgical processes. The nitrogen is mainly in solid solution which means that the nitrogen atoms appear randomly amongst the other atoms. Phosphorus in copper is also mainly in solid solution [12]. Both nitrogen in steels and phosphorus are elements that are diffusing faster than the dominating elements in the lattice. There are also major differences. Nitrogen in steels is present in interstitial positions, i.e. the N-atoms are located in between the positions in the face centred cubic (fcc) lattice. Phosphorus in copper on the other hand is substitutional. It replaces the copper atoms in the lattice. The content of nitrogen is of the order 10 to 40 times larger in 316LN than the phosphorus content in Cu-OFP. This is probably the main explanation why nitrogen has a pronounced effect on the tensile properties at room temperature. The yield strength increases linearly with nitrogen content. For phosphorus in copper no significant effect on the tensile properties is observed as pointed out above. The influence of nitrogen on creep properties is illustrated in Fig. 3.

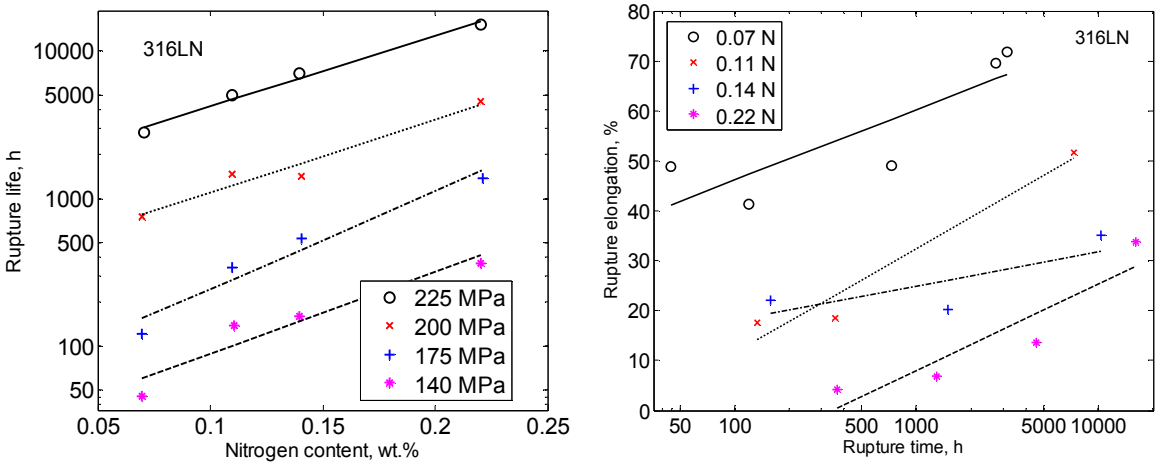

Fig. 3 Influence of nitrogen on creep properties of the austenitic stainless steel 316LN (17Cr-14Ni-2Mo) at 650ºC; a) Creep rupture life; b) Rupture elongation. From [13]

The rupture life increases with nitrogen content whereas the creep rupture elongation is reduced. The time dependence of the rupture elongation is shown in Fig. 3b and Fig. 4. Initially the elongation decreases with increasing rupture times. However, for very long rupture times, the elongation is approximately time independent. It has been demonstrated that the microstructure is essentially unchanged for long rupture times. For example, nitrides are not formed at long times.

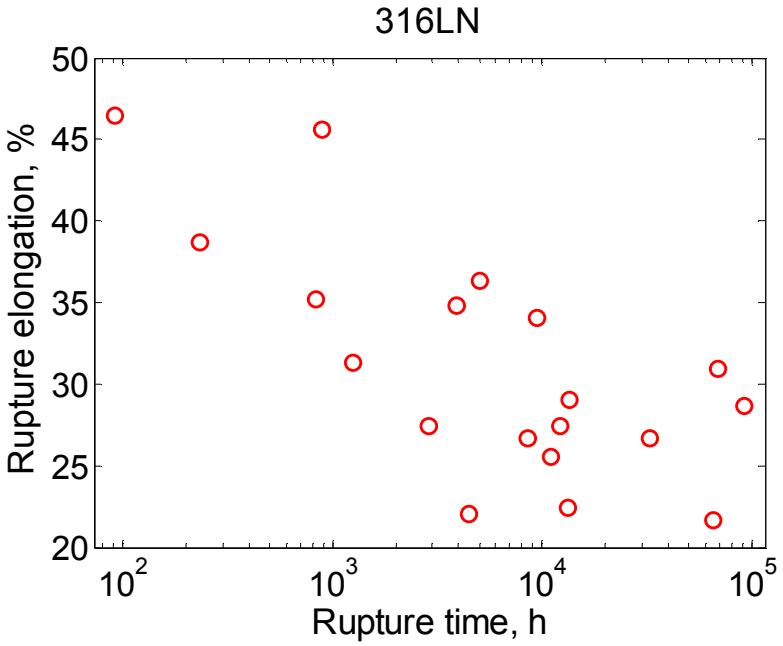

Fig. 4 Influence of nitrogen on creep rupture elongation of the austenitic stainless steel 316LN (17Cr-14Ni-2Mo-0.07N) at 550 ºC. From [14]

Several mechanisms have been proposed for the influence of nitrogen on creep strength [13].

Solid solution strengthening,
Four mechanisms may contribute to the solid solution strengthening

a) Pinning of dislocation by nitrogen atoms. This mechanism is probably quite important but it does not seem to have been analysed yet.

b) It is well known that the elastic modulus is influenced by the nitrogen content. For example, Mathew et al found that the modulus increased from 201 GPa for 0.07 wt.% N to 221 GPa for 0.22 wt.% [13]. However, from general principles for solid solution hardening, the resulting strength effect can be expected to be small [15].

c) Stacking fault energy. If the stacking fault energy is low it is difficult for the dislocations to climb, which slows down the creep rate [16]. Reduction in the stacking fault energy by addition of nitrogen has been observed for CrNi, CrNiMn, and NiMn steels [17]. This is quite a significant effect [16].

d) The formation of interstitial-solute complexes such as Cr-N have been found in nitrogen containing stainless steels [18]. If they have any effect on the strength is not known.

Precipitation hardening
Carbides such as $Cr_{23}C_6$ are formed at grain boundaries and at dislocations in austenitic stainless steels and give some contribution to the strength. Nitrides are only formed in special temperature intervals and play a less important role in this respect. Nitrogen is known to reduce the rate of coarsening of the carbides. This is a result of lowering the interface energy of the carbides [19]. This is most important because it means that the precipitation hardening survives to longer times.

Creep ductility
At long testing the creep damage appears at grain boundaries, resulting in rupture at the grain boundaries. The amount of creep damage decreased with increasing nitrogen content. [13]. This is probably the main reason why the rupture ductility takes an approximately constant value at longer times [14].

Comparison between Cu-OFP and nitrogen alloyed stainless steels
The mechanisms controlling creep strength and rupture ductility in Cu-OFP will be analysed in detail below. However, it is of interest at this stage to consider which of the mechanisms mentioned above for nitrogen alloyed stainless steels that are relevant for Cu-OFP. Out of the four mechanisms for *solid solution hardening* above only the first one is of importance, pinning of dislocations. The amount of phosphorus is too low to affect the elastic modulus [5]. With 1 wt.% P, the stacking fault energy is reduced [20]. However, for 50 wt.ppm, the effect is negligible. Since phosphorus is a substitutional element, mechanism d) is not relevant.

Since only a very limited number of phosphorus oxide and phosphate particles are formed for 50 wt.ppm [12], they do not give any significant *particle hardening*.

Detailed mechanisms for the influence of N on the *rupture ductility* of austentic stainless steels do not seem to have been proposed in the literature.

Why are basic models for creep deformation essential

For conventional pressure vessels, the design life is typically 10 to 30 years. According to the EU pressure equipment directive (PED), pressure vessels must be designed with formally approved materials, usually harmonised standard materials, which are referred to as pressure vessel approved materials. To get such approval, the prime requirement is that the material has adequate creep properties. For well established materials this implies in practice that the longest available creep testing times should reach about 70000 hours (8 years) [21], and that the material for such long rupture times should have adequate creep rupture ductility. The creep strength data is extrapolated to 200000 hours using statistical methods [21]. Due to their empirical nature, the extrapolation methods can not safely be used to longer times. Methods for extrapolation to longer times, so called extended extrapolation have been proposed, and have successfully been applied to some materials [22]. However, these methods have not yet been approved for pressure vessel standards. The resulting creep strength values are introduced in the pressure vessel codes and applied to design lives of up to 300000 hours (33 years). The creep rupture elongation values are not extrapolated because there are no general procedures available for this purpose.

An extrapolation of the creep strength by a factor of 3 to 4 in time is thus considered safe if a sufficient database can be accessed. For the copper canister two alternative design strategies can be considered

a) Creep tests are performed for up to 70000 hours and the creep strength is extrapolated in time by a factor of three to four. The measured creep rupture elongation values are used directly in design. This strategy corresponds to the established approach for the design of pressure vessels.

b) Fundamental models are developed for the controlling creep mechanisms. The models have to be quantitative and predictive, so they can be extrapolated to very long times.

Strategy a) would be applicable if the loading time in the repository would not exceed 300000 h. For many canisters this might well be the case, but low crack frequency rock could give much longer loading times until water saturation has been reached [2]. In

addition other load cases could also be of importance so that the canister can be exposed to creep for longer times. For example, earthquakes in connection with a retreating ice shield can give shear strains that induce stress relaxation for extended periods of time [9]. For these reasons, it is essential to develop fundamental models. Empirical deformation models are also available. Those models that are accurately adapted to existing plastic deformation and creep data can be used in predictions for loading times up to a few years. For longer loading times fundamental models have to be applied.

Part 2. Fundamental models for creep in copper

Mechanisms for influence of phosphorus on creep rupture strength

In metallic materials the linear defects called dislocations must be able to move to enable the material to deform plastically. Mechanisms to increase the strength are always based on ways to inhibit or slow down the motion of the dislocations. The phosphorus atoms must affect the dislocations in copper dramatically since a very low content of the element has such a pronounced influence. Thus, there is a strong interaction with the dislocations. This is illustrated in Fig. 5.

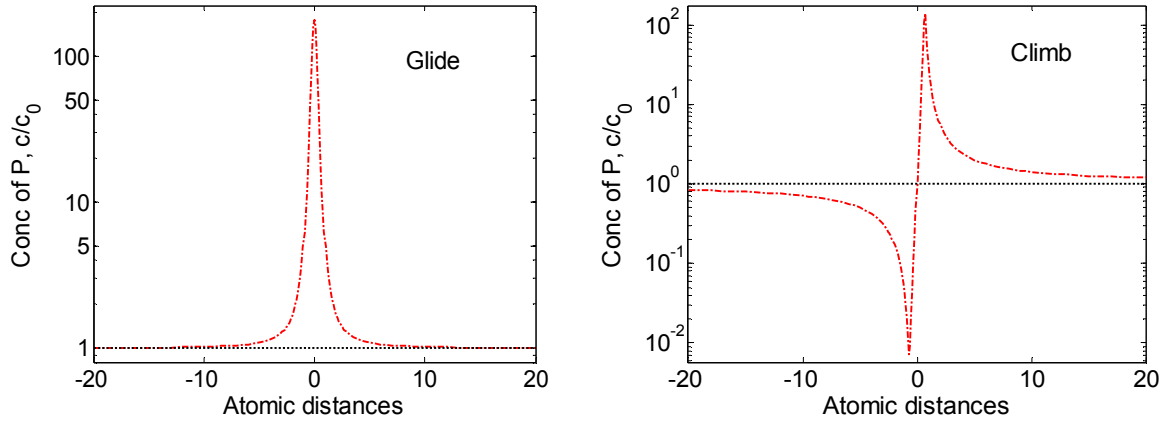

Fig. 5 Concentration of phosphorus as a function of distance from a dislocation expressed as the number of atomic distances. 75ºC; a) gliding dislocation; b) climbing dislocation. Redrawn from [23].

The concentration of phosphorus right at the dislocation core is more than 100 times larger than in rest of the material. This applies both to moving and stationary dislocations. The concentration of phosphorus atoms decreases somewhat with increasing temperature. The motion is most restricted for edge dislocations, which are built up by an extra half plane of atoms. The dislocation is the edge of the extra half plane, and that is the reason for its name, Fig. 6. Two main mechanisms for the motion of the dislocations are considered: glide and climb. Glide occurs in a direction perpendicular to the extra half plane. Glide takes place readily because no transport of atoms is required. The climb motion is in the extra half plane perpendicular to the edge. For climb to occur, diffusion of atoms to and from the dislocation must take place, which is a slow process. The maximum concentration of phosphorus is about the same for glide and climb of dislocations, Fig. 5.

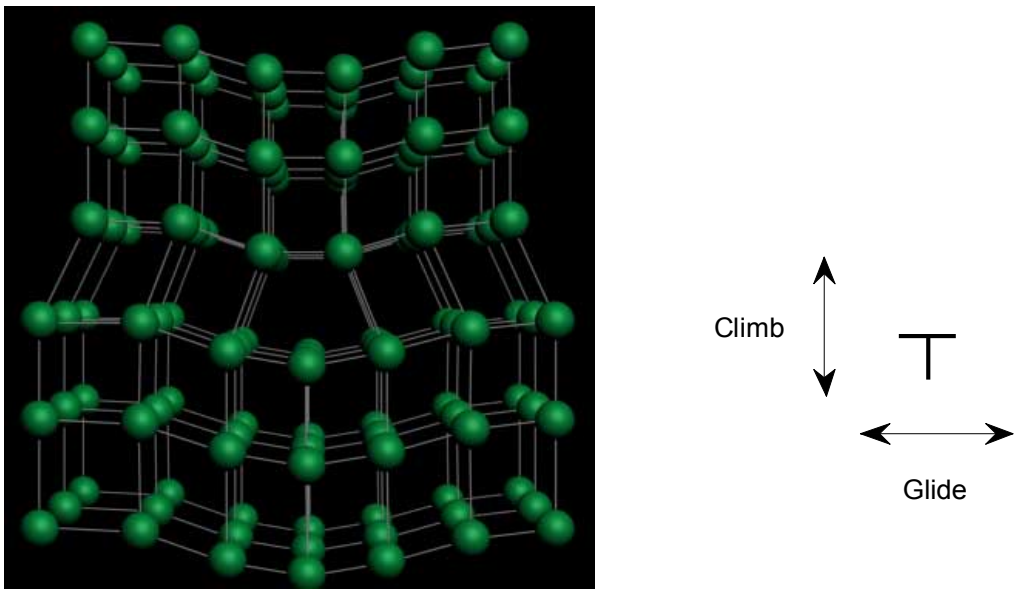

Fig. 6 Illustration of atom positions around an edge dislocation with its extra half plane at the centre of the lower half of the left hand image. The climb and glide directions are marked.

The concentration of solute atoms at the dislocations is often referred to as Cottrell atmospheres. When dislocation moves the atmosphere of atoms try to follow. This slows down the motion of the dislocations, which is equivalent to a force acting against the motion. This so called solute drag effect gives a contribution to the strength. In [23] the size of the solute drag effect is computed. It turns out that the effect is quite small, less than 1 MPa, which is negligible. For this and other models, the access to accurate thermodynamic and diffusion data is essential [12], [24].

The concentration profiles in Fig. 5 are quite sharp. 90% of the P atoms are within one atomic distance from the core of the dislocation. Fig. 5 is based on the assumption that the P atoms can be placed at any distance from the core. This is of course not possible, since the P atoms must be placed at the positions in the crystal lattice. Apart from the position at dislocation cores, the closest is one atomic distance (one Burgers vector) away. When the dislocations move this has quite important consequences. After a dislocation has moved one atomic distance, the majority of the P atoms are suddenly outside the distributions illustrated in Fig. 5. Although this is a somewhat simplified argument, it is clear that the dislocation has to break away from the P atoms to move. This corresponds to a break stress, which is about 23 MPa at 75ºC [23]. Taking this value into account in the expression for the creep rate for Cu-OF [25], the values for Cu-OFP can be reproduced. This is illustrated in Fig. 7.

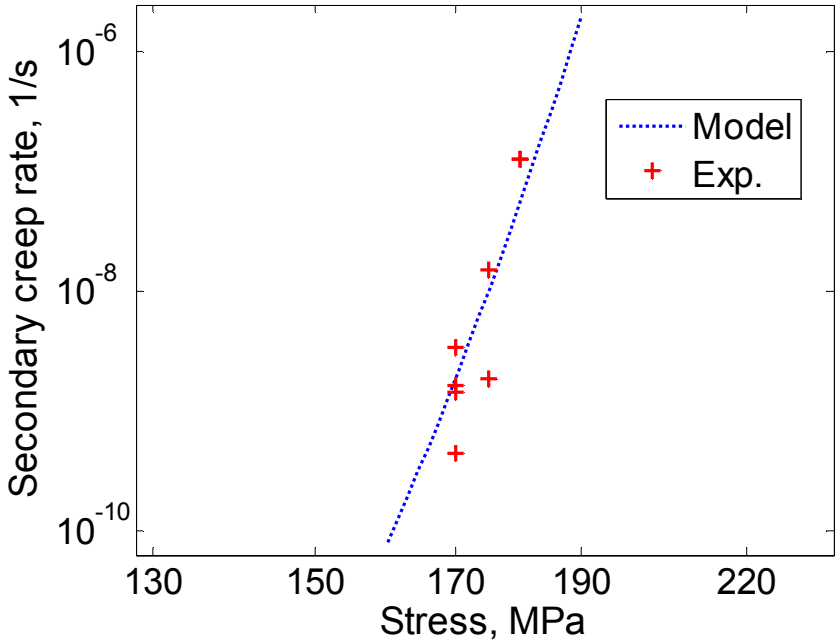

Fig. 7 Secondary creep rate versus stress for Cu-OFP at 75ºC. Adapted from [26].

In this way a detailed explanation of the influence of phosphorus has been found. Unfortunately, it is not fully quantitative since the results are sensitive to the nature of the core region of the dislocations, which is not fully known. To handle this situation an assumption has been made about the influence of phosphorus, an assumption about the creep rate ratio between Cu-OF and Cu-OFP that has been found to be valid even for extrapolation to very long times [26].

Creep strain predictions

In references [26] and [27] a general dislocation model for plastic deformation of copper is formulated. Three processes are taken into account: work hardening, dynamic recovery and static recovery. The work hardening describes how the hardness of the material increases when it is exposed to plastic deformation. New dislocations are generated and create a "forest" that makes it more difficult for other dislocations to move, i.e. the strength is raised. When the dislocations are transported during the deformation, they sometimes hit dislocations with opposite Burgers vectors and are eliminated. This is called dynamic recovery and it reduces the density of dislocations and makes the apparent work hardening lower. The dislocations can also interact during a heat treatment without any plastic deformation. Dislocations with opposite Burgers vectors attract each other and when they meet, they annihilate. This is referred to as static recovery. So there is one process (work hardening) that creates dislocations and one deformation controlled process (dynamic recovery) as well as one time dependent process (static recovery) that eliminate them.

If the expressions for the three processes are combined most interesting results can be obtained. If the *work hardening and the dynamic recovery* are considered, a well established expression for stress strain curves in copper is obtained, the Kocks-Mecking equation [27]. This equation can describe measured tensile stress strain curve quite accurately. Two cases are illustrated in Fig. 8

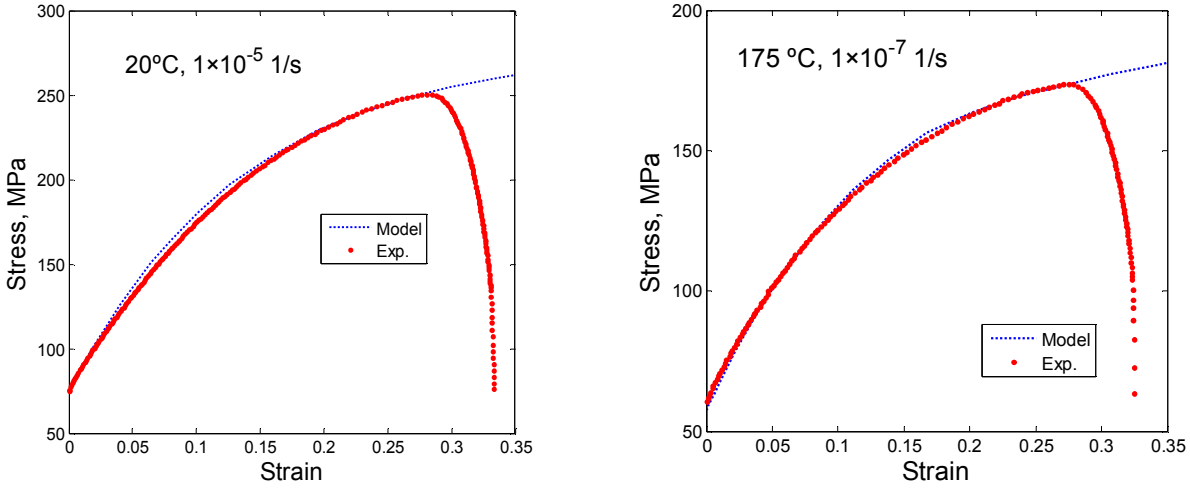

Fig. 8 Comparison of experimental and model values for tensile stress strain curves for Cu-OFP; a) 20ºC, 1×10^{-5} 1/s. b) 175ºC, 1×10^{-7} 1/s. From [27]

The model predicts the strain curves until the instability starts, i.e. when a waist is formed on the specimen. At this stage the experimental curves rapidly bend downwards.

If instead *work hardening and recovery* are assumed to balance, an equation for the secondary creep rate is obtained. The use of this equation is illustrated in Fig. 7.

Finally if the *Kocks-Mecking equation* is combined with the *expression for the secondary creep rate*, the creep strain versus time can be described. This application is illustrated Fig. 9. For simple uniaxial specimens, the primary and secondary part can represent experimental values for temperatures from 75 to 250ºC [26], Fig. 9a. The expression takes into account the initial stage of the creep curve when the slope of the curve (creep rate) is decreasing (primary creep) and the secondary stage where the creep rate is constant. The final tertiary stage when the creep rate is increasing is not covered by the model. The model can be generalised to multiaxial stress states. This is shown in Fig. 9b where the results for a notched specimen are given.

It is obvious that a basic model for plastic deformation can handle several different types of mechanical tests. It can describe plastic deformation at least approximately for a wide range of testing conditions. It has been demonstrated this also include very low stresses that can appear in the canister [26]

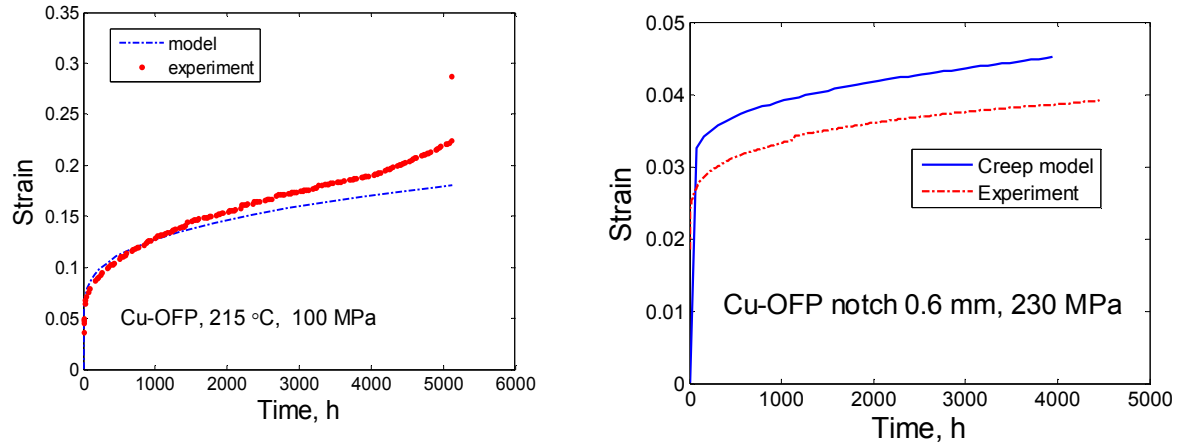

Fig. 9 Comparison of experimental and model values for creep strain versus time curves for Cu-OFP; a) 215ºC, 100 MPa, straight uniaxial specimen. b) 75ºC, 230 MPa, notched round specimen. From [26]

Creep in weldments

In common types of high temperature plants such as fossil fired power plants, the creep damage is often localised to the weldments. The welds appearing between the lid and the canister tube and for extruded tubes also between the tube and the base of the canister are consequently of importance to investigate with respect to possible presence of creep damage.

For this purpose the basic model has been generalised to cover the different zones in friction stir welds, which is the type of welding that is planned to be used. The friction stir welds consist of two zones: the thermo-mechanically affected zone (TMAZ) that is in the centre of the weld and the heat affected zone (HAZ) that surrounds TMAZ. A schematic illustration of the weld zones is given in Fig. 13 below.

Tensile and creep properties have been determined for the two zones TMAZ and HAZ and for specimens that include more than one zone (cross-weld specimens) [28]-[31]. The results demonstrate that the tensile flow curves are slightly higher than for the parent metal, i.e. the strength of the weld zones is higher. On the other hand the two weld zones creep faster than the parent metal at the same conditions [32]. The creep strength for the weld zones is thus slightly lower than for the parent metal.

Constitutive equations have been developed for the weld zones for both tensile flow curves and creep strain versus time curves. In comparison to the corresponding models for base metal, only one change has been made. If the dislocations get close enough and are of opposite sign they will attract each other and eventually they combine and are eliminated. For the parent metal the distance when this takes place was derived to 2.5 Burgers vectors [27]. Since the microstructure is more complex in the weld zones than in the base metal, it is reasonable to assume that the interaction distance is smaller in the welds. The value for the interaction distance for the weld zones has been taken as 2 Burgers vectors [31]. This is the smallest possible value, since the distance can not be lower than twice the dislocation core radius. With this assumption observed tensile flow curves and creep strain versus time curves can be reproduced.

This is illustrated in Fig. 10 for the tensile flow curves. One example for TMAZ and one for HAZ are given. A significant variation in the flow curves between tests was observed. This variation was carefully analysed. It was found that the local properties of the

weldments showed this effect [31], so it was not a result of method used in the measurements.

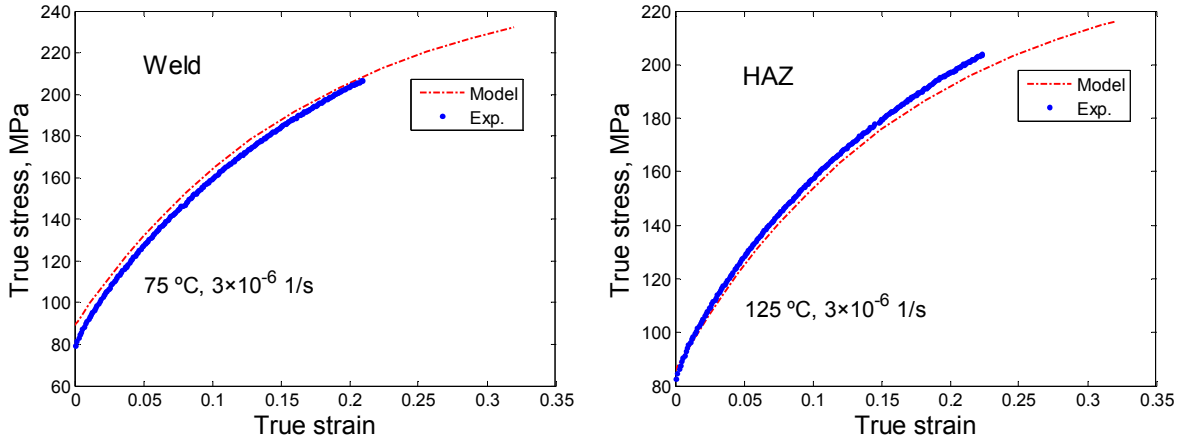

Fig. 10 Comparison of experimental and model values for tensile stress strain curves for weld zones in Cu-OFP; a) Weld (TMAZ) 75ºC, 1×10^{-6} 1/s. b) HAZ, 125ºC, 3×10^{-6} 1/s. From [31].

Creep strain curves for the two weld zones are presented in Fig. 11. The cusps on the experimental curves are due to the necessity of reloading the creep machine one or more times.

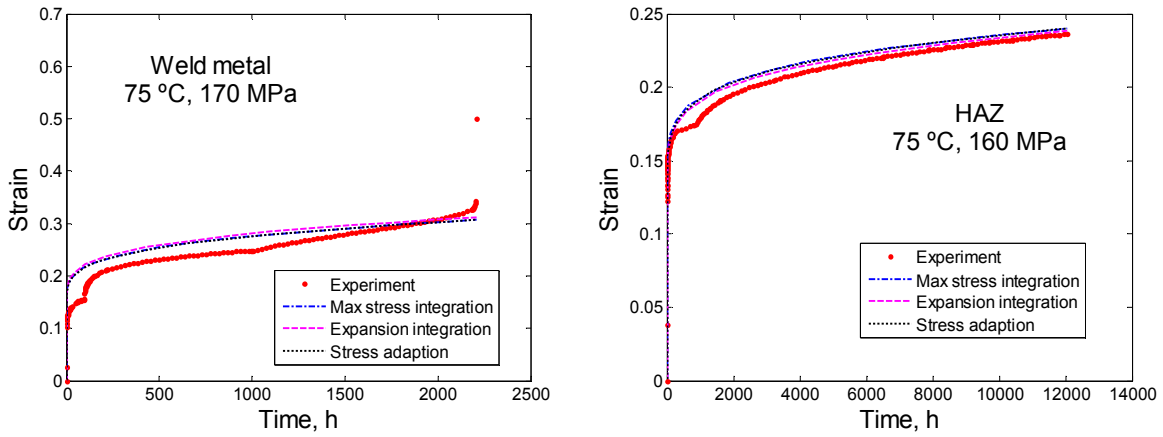

Fig. 11 Comparison of experimental and model values for creep strain versus time curves for weld zones in Cu-OFP; a) Weld (TMAZ) 75ºC, 170 MPa; b) HAZ 75ºC, 160 MPa. From [31]

The developed model for the weld zones has been transferred to constitutive equations that can be applied in finite element analysis (FEA). Three different approaches have been formulated Max stress integration, Expansion integration and Stress adaptation. It is demonstrated in Fig. 11 that they give the same result (as they should). When FEA is performed the most practical one from the computational point of view can be chosen.

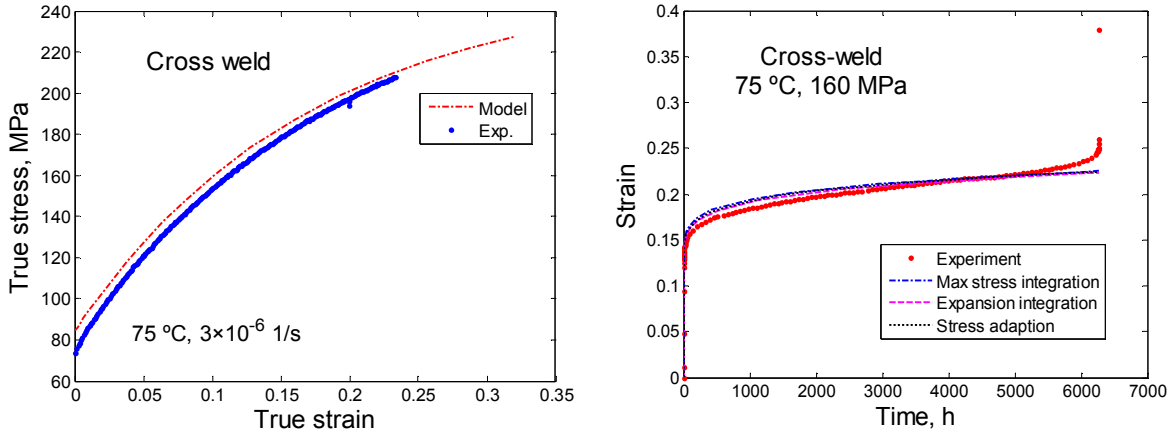

Fig. 12 Results for cross welds for Cu-OFP; a) Tensile flow curve 75ºC, 3×10^{-6} 1/s. b) Creep strain versus time curve 75ºC, 160 MPa 1/s. From [31]

In Fig. 12 it is demonstrated that the behaviour across weldments (cross welds) can be described. The cross welds include TMAZ, HAZ and base metal.

Welds in the canister

Using the constitutive equations, the stresses and strains around the weldments in the canister have been analysed with finite element methods [33]. The different properties in the base metal, TMAZ, and HAZ are taken into account. In the repository,it is expected that the canister will be exposed to a gradually increasing external pressure. The maximum pressure represents the situation when the bentonite clay is fully water saturated. The time scale for this pressure can probably vary significantly between individual canisters. In the computation results that are shown below, it has been assumed that a gradual loading over a time period of one year takes place, which is at the lower end of the loading time spectrum.

Fig. 13 illustrates the stress distribution around the bottom and top weldments in the canister (von Mises stress). The stresses in the heat affected zone (HAZ) are fairly constant and take values of about 90 MPa in both welds. The creep rate that such a stress level would give rise is negligibly small [30]. The stress is also fairly constant outside the HAZ. The stress level is about 65 MPa. In the thermomechanically affected zone (TMAZ) inside the parabolas, the stress is also fairly homogeneous with a value of 85 MPa or below.

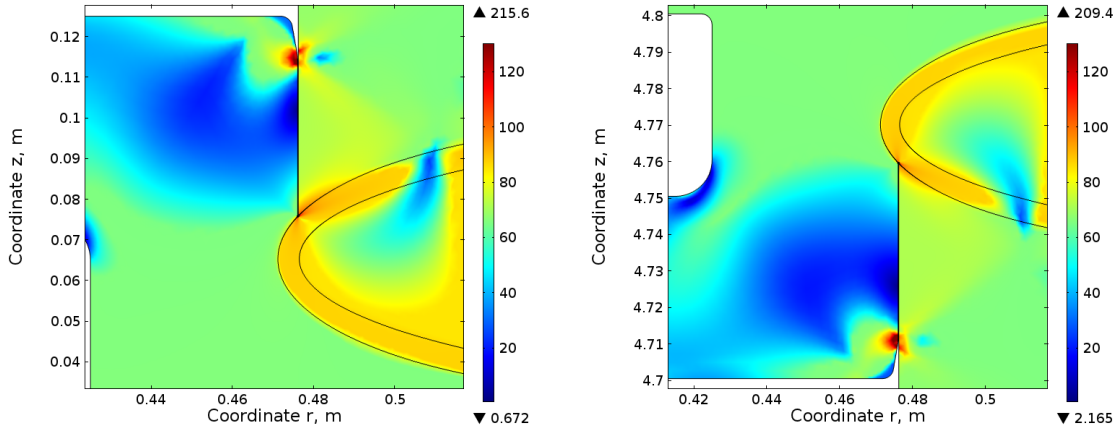

a) b)

Fig. 13 von Mises stress (MPa) in and around the weld zones for load case 0; a) base weld; b) lid weld. The weld is represented by an inner parabolic area, the thermomechanically affected zone, TMAZ, and a surrounding about 5 cm wide parabolic region, the heat affected zone, HAZ. From [33].

The low stress levels around the weldments give only rise to low strains, less than 5%, Fig. 14.

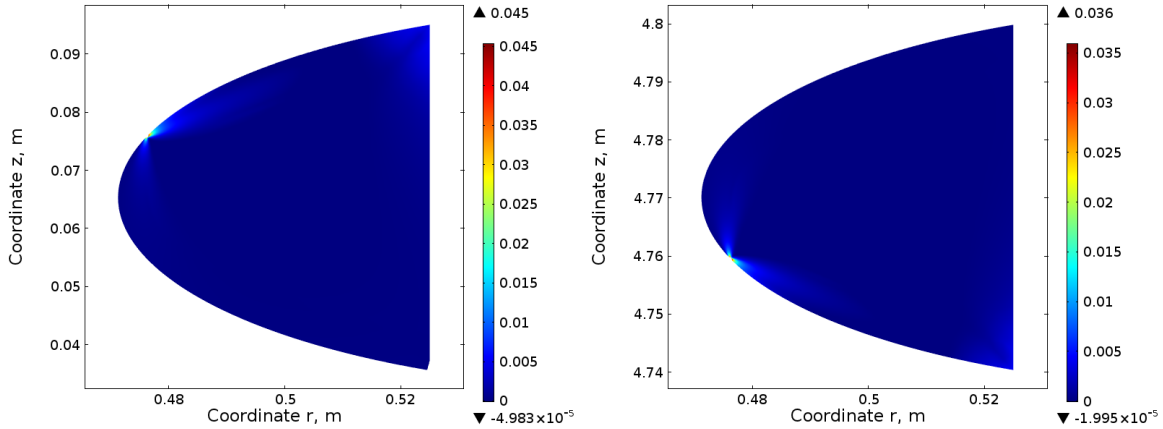

a) b)

Fig. 14 . Plastic strain distribution for the welds for load case 0; a) base weld; b) lid weld.

The stresses and strains in Fig. 13 and Fig. 14 are comparatively small and will not threaten the integrity of the canister. The intersections between the lid and canister tube and between the base and canister tube are referred to as the slits. In the bottom of the slits the stresses and strains can be quite high. This is illustrated for the upper slit root in Fig. 15.

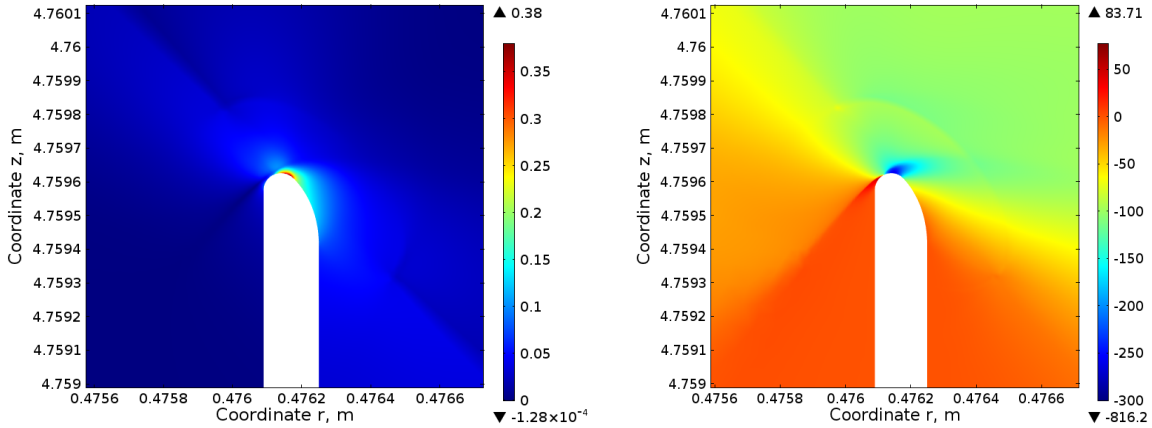

a) b)

Fig. 15 Upper slit root; a) plastic strain distribution; a) radial stress component, which is perpendicular to the slit.

The maximum strain in the slit roots can exceeds 0.3 (30%). However, the size of these zones is less than 20 µm. This is too small to make a crack propagate. Furthermore, the stresses are compressive perpendicular to the slits in these zones, Fig. 15b.

Cavitation

During creep deformation, cavities are formed at the grain boundaries. The grains move relative to each other. This is called grain boundary sliding. This sliding gives rise to the formation of creep cavities. With increasing strain, the number of cavities increases. At the same time the cavities grow in size. Eventually a fraction of the grain boundaries is covered by cavities and rupture will occur. In the modelling it is assumed that this takes place when the cavitated area fraction is 25% . The exact value chosen is not critical for the prediction of the time to rupture, since the cavitated area fraction increases very rapidly near the end of creep life.

It was observed a long time ago that the number of creep cavities is approximately proportional to the creep strain in copper [34]. The same behaviour is also observed for steels [35]. The amount of grain boundary sliding is proportional to the creep deformation [36]. In the computations a value measured in tensile tests have been used [37]. That the amount of grain boundary sliding is proportional to the creep deformation is consistent with the common assumption that the nucleation of cavities is controlled by grain boundary sliding. The cavities are nucleated at inhomogeneities in the grain boundaries, such as inclusions and other particles [38]. Nucleation is also observed when aggregations of dislocations in the form of cell and subgrain boundaries meet the grain boundaries [39]. Since particles are infrequent in Cu-OFP, it is assumed in the modelling that the dislocation substructure controls the nucleation. More precisely it is assumed that when two subboundaries on different sides of the grain boundaries meet during boundary sliding, a cavity is formed. With these assumptions a quantitative model for the nucleation of cavities has been set up [7].

Contrary to the situation for nucleation, well established equations for the growth of cavities exist. In particular for copper, the validity of the equations have been demonstrated a number of times [7]. Two main contributions to the growth of cavities are considered: from diffusion and from creep strain. For cavities that are located at grain boundaries perpendicular to the loading direction, there is a driving force to expand since this contributes to the elongation of the specimen. As a consequence there is an energy gain if

vacancies are diffusing to these cavities. This is the basis of diffusion growth. An expression for this type of growth can be found in [40]. This expression has been used for copper in several papers [7]. The second contribution is due to the deformation of the cavities. In its simplest form it is assumed that the length of the cavities in the straining direction is proportional to the creep strain [41]. This gives a comparatively small contribution to the cavity growth. However, if the influence of stresses in more than one direction (multiaxiality) is taken into account, the contribution can be quite significant. In the modelling the approach by Rice and Tracey has been used [7], [42]. Alternative approaches exist, but the one proposed in [42] has been chosen since it has given the most stable solution. As proposed by Beere [40], the two contribution have been added to find the total growth rate [7].

It is evident from Fig. 1 that phosphorus has a large influence on the creep rupture and thus also on the cavitation for Cu-OF, since cavitation initiates the rupture at the grain boundaries. Several possible mechanisms for this influence has been analysed. There is a strong interaction between phosphorus and the grain boundaries [43]. As a consequence phosphorus is accumulating at the grain boundaries. The interaction between phosphorus and the grain boundaries is likely to affect grain boundary sliding, the local creep deformation, as well as the motion of dislocations in the grain boundaries. These processes influence the cavitation by reducing the stress that controls the cavity nucleation and growth [7]. Which of these mechanisms that is the main one is investigated at present by SKB. However, estimates suggest that their influence is quite similar. It is clear that the strong interaction between phosphorus atoms and the grain boundaries is the origin of the reduced amount of cavity formation in phosphorus containing copper, and this explains why the creep ductility is so much improved in this type of material.

When models for both nucleation and growth are available, creep rupture can be predicted. A distinction is made between ductile and brittle rupture. Ductile rupture is assumed to be due to creep strain exhaustion. When the creep strain exceeds the tensile elongation, ductile rupture takes place. The critical elongation has been chosen to 0.4 (40%) [7]. The brittle rupture is due to cavitation in the grain boundaries. As pointed out above the critical value for the cavitated area fraction has been set to 0.25 (25%). The final rupture occurs when the first of the rupture criterion has been reached. The predicted rupture times are illustrated in Fig. 16. It is evident that a description of the general rupture behaviour has been obtained.

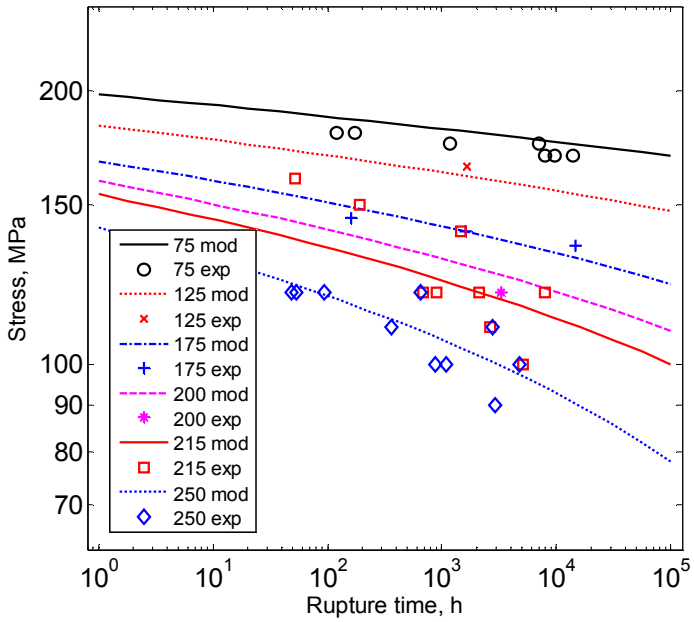

Fig. 16 Creep stress versus rupture time for Cu-OFP for temperatures from 75 to 250 ºC. The model values are computed as the time when the first of ductile and brittle rupture occurs. From [44].

In addition to the time when the rupture occurs, the creep strain is obtained. This is the creep rupture elongation. The creep rupture elongation does not depend very much on the rupture time, Fig. 2b. For this reason, observed rupture elongation values have been plotted as a function of temperature, Fig. 1b. For Cu-OF brittle rupture is predicted for the covered temperature range whereas for Cu-OFP the rupture is ductile. The model can reproduce the experimental values quite well for both Cu-OF and Cu-OFP. If the model values are extrapolated to long times, the predicted rupture is still ductile for Cu-OFP and high rupture elongation values are obtained.

Creep crack growth

If notches or cracks are present during creep they could give rise to creep crack growth. For this reason creep crack growth has been studied with the help of fracture mechanics specimen, where a deep crack is present at the start of the test. A load is applied perpendicular to the crack plane. If the material is sensitive to creep crack growth, the crack will start to grow after an initial time. Tests have been performed at 20, 75, 175 and 215ºC [44]. The tests at 175 and 215ºC showed pronounced creep crack growth and ruptured after fairly short time. However, the tests at 20 and 75ºC did not show any crack growth in spite of the fact that tests were run up to 10000 h (1.1 years). These tests had side notches (side grooves) to enhance the effect of multiaxiality. Tests at 75, 100, 125, and 175ºC without side grooves are in progress and have run between 2000 and 12000 h. For these specimens no creep crack growth has been observed.

With the help of finite element analysis, the stress state in front of the crack has been computed. This stress state has been applied in the cavitation model discussed in the previous section for the different specimens. The crack is assumed to propagate when one of the two rupture criteria is fulfilled. In the modelling of the creep crack growth, exactly the same model parameters and the same rupture criteria has been used as for the results in Fig. 1 and Fig. 16. Only the conditions corresponding to the tests at 175 and 215ºC with

side growths gave any crack propagation. The computed crack propagation for these cases is presented in Fig. 17.

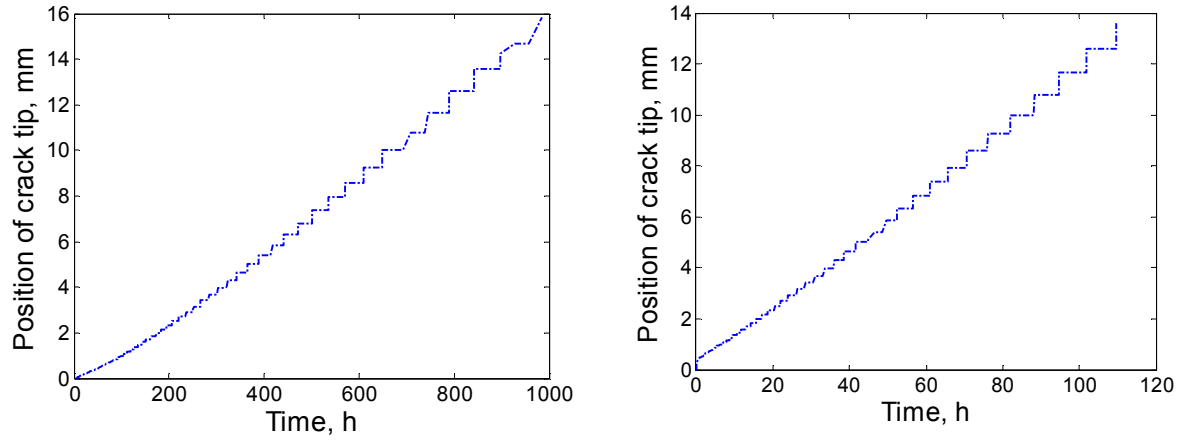

a) b)

Fig. 17 Simulated crack tip position versus time at conditions corresponding to tests; a) 175 ºC, test failed after 812 h; b) 215 ºC, test failed after 121 h. From [44].

The development of the crack length could not be measured during the test because the resistivity across the crack was too low to allow recording of changes in the electrical potential (potential drop). The total crack length was, however, about 15 mm. Although the overall result in Fig. 17 seems quite satisfactory, a real crack can be expected to progress in a more stepwise way. The development of the creep damage during a test when the crack propagates and the distance from the original crack tip increases is illustrated in Fig. 18.

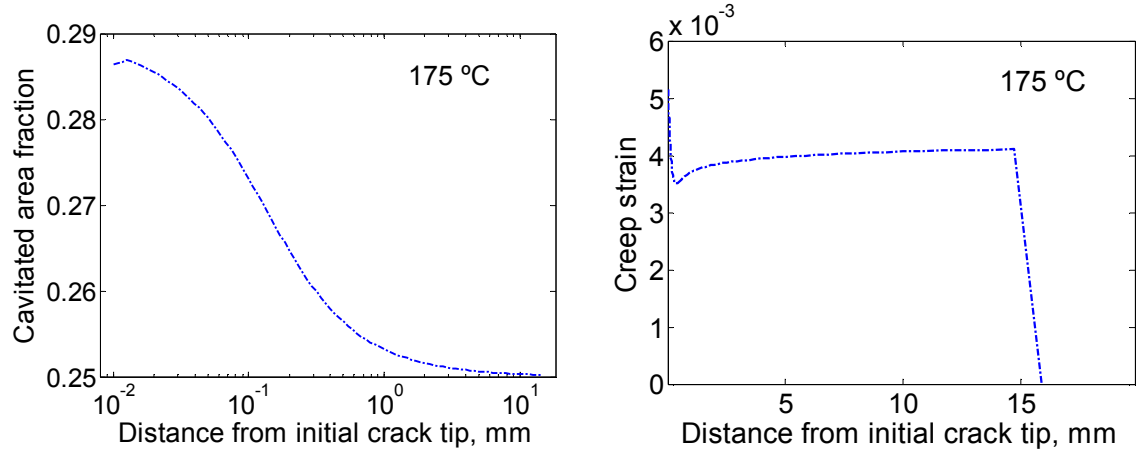

Fig. 18 Creep damage at the crack tip versus tip position. Simulated test at 175 ºC with a failure time of 812 h; a) cavitated area fraction (log length scale); b) creep strain (linear length scale). From [44].

The test in Fig. 18 is associated with brittle rupture. This means that the crack propagation is controlled by the cavitated area fraction, which is close to the assumed critical value of 0.25 (25%). Initially the cavitated area fraction is even higher before stationary conditions have been reach. The creep strain at the crack tip is much smaller than the critical value of 0.4, and the creep strain does not affect the crack propagation.

Deep notches are present in the slits in the canister between the canister tube and lid and between the tube and base. As pointed out above the local effective strains seem to be high enough to initiate creep crack growth. However, this is not possible for two reasons. First, the regions with critical strains have an extent less than 20 μm. The size of the region must be at least equal to the grain size ($\geq$ 70 μm) to make the crack move from the creep damage in one grain boundary to the damage in the next [33]. Second, the first principal stress in the region is compression which makes it impossible for the creep damage to develop [7], [33].

Concluding remarks

The strong influence of phosphorus in the ppm range on creep properties seems to be unique, and the controlling mechanisms have now (after a number of years) been identified based on the accumulation of phosphorus atoms at the dislocations and at the grain boundaries. Another challenge has been the development of fundamental models for creep strength, creep deformation and creep ductility. This has now been accomplished. These models allow the prediction of properties for very long times. With the models the temperature, stress and time dependence can be handled. The models have and will be applied to FEM analysis of the design of the canister. This includes for example normal loads in the repository as well as shear loads in case of earthquakes. Empirical deformation models are also available. Those models that are accurately adapted to existing plastic deformation and creep data can be used in predictions for loading times up to a few years. For longer loading times the fundamental models are applied.

References

[1] Unfired pressure vessels, European standard EN 13445-2:2002, Issue 35 (2009-01)

[2] Long-term safety for the final repository for spent nuclear fuel at Forsmark. Main report of the SR-Site project. Updated 2012-12. SKB Technical Report TR-11-01, section 10.3.8 (2011)

[3] Henderson P. J., Österberg J. O., Ivarsson B., Low temperature creep of copper intended for nuclear waste containers. SKB Technical Report TR 92-04 (1992).

[4] Sandström R,. Henderson P. J. "Low temperature creep ductility of OFHC copper", Materials Science and Engineering A (Switzerland). Vol. 246, no. 1-2, pp. 143-150 (1998)

[5] Metals Handbooks, Vol 2, 9th edition. Properties and selection: nonferrous alloys and pure metals, American Society for Metals, Metals Park (1979)

[6] Butomo DG, Zedin NI, Mnushkin OS. Effect of oxygen on the susceptibility of copper to "hydrogen sickness". Met Sci Heat Treat. 1968;10:184-5.

[7] Sandström R, Wu R. Influence of phosphorus on the creep ductility of copper. J Nucl Mater. 2013;441:364-71.

[8] Sandström R. Extrapolation of creep strain data for pure copper. J Test Eval. 1999;27:31-5.

[9] Raiko H, Sandström R, Rydén H, Johansson M. Design analysis report for the canister. Swedish Nuclear Waste Management Company Technical Report TR 10-28; 2010.

[10] Andersson-Östling, HCM, Sandström, R, Survey of creep properties of copper intended for nuclear waste disposal, SKB Technical report TR-09-32 (2009)

[11] Perry M, Morris PF, Clarke PD. Optimisation of the long-term service performance of Durehete 1055 bolting steel. Mater High Temp. 2010;27:45-52.

[12] Magnusson H, Frisk K. Thermodynamic evaluation of Cu-H-O-S-P system. Phase stabilities and solubilities for OFP-copper. Swedish Nuclear Waste Management Company Technical Report TR-13-11, 2013.

[13] Mathew MD, Laha K, Ganesan V. Improving creep strength of 316L stainless steel by alloying with nitrogen. Materials Science and Engineering A. 2012;535:76-83.

[14] Takahashi Y, Shibamoto H, Inoue K. Long-term creep rupture behavior of smoothed and notched bar specimens of low-carbon nitrogen-controlled 316 stainless steel (316FR) and their evaluation. Nuclear Engineering and Design. 2008;238:310-21.

[15] Sieurin H, Zander J, Sandström R. Modelling solid solution hardening in stainless steels. Mat Sci Eng A. 2006;415:66-71.

[16] A.S. Argon, W.C. Moffatt, Climb of extended edge dislocations, Acta Metallurgica 29, Issue 2, February 1981, Pages 293-299

[17] Schramm RE, Reed RP. Stacking fault energies of seven commercial austenitic stainless steels. Metallurgical Transactions A. 1975;6:1345-51.

[18] Oda K, Kondo N, Shibata K. X-ray Absorption Fine Structure analysis of interstitial (C, N)-substitutional (Cr) complexes in austenitic stainless steels. ISIJ International. 1990;30:625-31.

[19] Lai JKL. A review of precipitation behaviour in AISI type 316 stainless steel. Materials Science and Engineering. 1983;61:101-9.

[20] Sztwiertnia K. On recrystallization texture formation in poly crystalline fee alloys with low stacking fault energies. International Journal of Materials Research. 2008;99:178-90.

[21] ECCC Recommendations Volume 5 Part 1a, 'Generic recommendations and guidance for the assessment of full size creep rupture datasets', Issue 5 (2003), ed. Holdsworth, SR., publ. ETD, www.ommi.co.uk/etd/eccc/advancedcreep.

[22] Sandström R. A procedure for extended extrapolation of creep rupture data. J Test Eval. 2003;31:58-64.

[23] Sandström R, Andersson HCM. The effect of phosphorus on creep in copper. J Nucl Mater. 2008;372:66-75.E

[24] Magnusson H, Frisk K. Self-diffusion and impurity diffusion in the hydrogen, oxygen, sulphur and phosphorous in copper. Swedish Nuclear Waste Management Company Technical Report TR-13-24; 2013.

[25] Sandström R, Andersson HCM. Creep in phosphorus alloyed copper during power-law breakdown. J Nucl Mater. 2008;372:76-88.

[26] Sandström R. Basic model for primary and secondary creep in copper. Acta Mater. 2012;60:314-22.

[27] Sandström R, Hallgren J. The role of creep in stress strain curves for copper. J Nucl Mater. 2012;422:51-7.

[28] Andersson HCM, Seitisleam F, Sandström R. Creep testing of thick-wall copper electron beam and friction stir welds. Materials Research Society Symposium Proceedings 2004. p. 51-6.

[29] Andersson HCM, Seitisleam F, Sandström R. Creep testing of thick-wall copper electron beam and friction stir welds at 75, 125 and 175ºC. Swedish Nuclear Waste Management Company Report TR-05-08; 2005.

[30] Andersson HCM, Seitisleam F, Sandström R. Creep testing and creep loading experiments on friction stir welds in copper at 75 °C. Swedish Nuclear Waste Management Company Report TR-07-08; 2007.

[31] Sandström R, Waqas Ahmad S, Pasupuleti KT, Mahdavi Shahri M. Slow strain rate tensile testing of friction stir welded Cu-OFP. Constitutive equations for creep. Swedish Nuclear Waste Management Company Technical Report R-13-33; 2013.

[32] Sandström R, Östling H, Jin LZ. Modelling of creep in friction stir welded copper. Materials Research Innovations. 2013;17:350-4.

[33] Jin LZ, Sandström R. Influences of load variations on the plastic deformation in friction stir welds and contour slits in copper canisters Swedish Nuclear Waste Management Company Technical Report TR-13-25; 2013.

[34] Needham NG, Wheatley JE, Greenwood WG. The creep fracture of copper and magnesium, Acta Metallurgica 23 (1975), pp 23-27

[35] Wu R, Sandstrom R. Strain dependence of creep cavity nucleation in low alloy and 12%Cr steels. Mater Sci Tech Ser. 1996;12:405-15.

[36] Mclean D, and Farmer M.H. The relation during creep between grain boundary sliding, sub-crystal size and extension, J. Inst. Metals 85 (1956) 41-50

[37] Pettersson K. A study of grain boundary sliding in copper with and without an addition of phosphorus. J Nucl Mater. 2010;405:131-7.

[38] Evans RW., Wilshire B., Introduction to Creep, The Institute of Materials, London, UK, 1993.

[39] Lim LC. Cavity nucleation at high temperatures involving pile-ups of grain boundary dislocations. Acta Metallurgica. 1987;35:1663-73.

[40] Beere W. Cavities and Cracks in Creep and Fatigue (edited by J. Gittus). Applied Science, New York, (1981)

[41] Davanas K, Solomon AA. Theory of intergranular creep cavity nucleation, growth and interaction. Acta Metallurgica Materialia. 1990;38:1905-16.

[42] Rice JR, Tracey DM. On the ductile enlargement of voids in triaxial stress fields. Journal of the Mechanics and Physics of Solids. 1969;17:201-17.

[43] Korzhavyi PA, Johansson B, Lozovoi AY. Segregation of 3sp impurities to Σ5(310) tilt grain boundary in copper, Swedish Nuclear Fuel and Waste Management Co, Technical Report TR-01-25, pp. 32-39, Stockholm, 2001,

[44] Wu R, Sandström R, Jin LZ. Creep crack growth in phosphorus alloyed oxygen free copper. Materials Science and Engineering A. 2013;583:151-60.